

Electron focusing by multiple-quantum-point contacts

This article has been downloaded from IOPscience. Please scroll down to see the full text article.

1992 J. Phys.: Condens. Matter 4 7121

(<http://iopscience.iop.org/0953-8984/4/34/011>)

View [the table of contents for this issue](#), or go to the [journal homepage](#) for more

Download details:

IP Address: 171.66.16.96

The article was downloaded on 11/05/2010 at 00:27

Please note that [terms and conditions apply](#).

Electron focusing by multiple-quantum-point contacts

K Michielsen and H De Raedt

Institute for Theoretical Physics, University of Groningen, Nijenborgh 4, NL-9747 AG Groningen, The Netherlands

Received 8 May 1992, in final form 1 July 1992

Abstract. A device for focusing ballistic electrons is proposed. It consists of an array of quantum point contacts and a potential barrier drawn up by a gate. Computer simulation analysis of this device shows that it can focus electrons in a cone of 20° , with a throughput of $\approx 0.6\%$.

Recent progress in manufacturing nanometre structures in two-dimensional electron gas (2DEG) systems have made it possible to perform 'electron-optics' experiments in solid-state devices [1]. In an ideal device the motion of the electrons is not affected by interactions with impurities, phonons etc, i.e. the electrons travel ballistically, just as they would do in ultra-high vacuum. In real devices, typical distances for ballistic motion can be as large as $250\lambda_F$, λ_F being the Fermi wavelength of the electrons [2]. If the dimension of the point contacts becomes comparable to λ_F , a classical 'billiard-ball', treatment of the motion of the electrons is no longer valid. To explore the properties of electron transport through quantum point contacts a proper, wave-mechanical, description is required.

The ability to focus a beam of light by means of lenses is very important for a wide variety of applications and this holds for the focusing of electrons as well [3]. In solid-state devices, the electrons emerging from the quantum point contact can be directed to a small area by applying a magnetic field [2], by putting a gate behind the point contact [4, 5] or by refraction of the electrons by a convex lens (i.e. a region in which the electrons have a longer wavelength) [6].

In this paper we propose a device which focuses the electrons in a cone of 20° or less, is controlled by a gate and has a high throughput, thereby alleviating most of the shortcomings [3] of the above-mentioned focusing techniques. The layout of the device is depicted in figure 1. Several quantum point contacts are put in parallel to form a grating. The grating is followed by a tunnelling barrier (drawn up by a gate). The height of the barrier is to be chosen such that it is slightly below the Fermi energy E_F . To be concrete we consider a 'typical' grating of thickness λ_F , period $a + b = 2\lambda_F$ and linewidth $b = \lambda_F$.

To investigate the focusing capability of the device we envisage the following thought experiment. Imagine a wave, with a well-defined direction and energy E_F , impinging on the grating+barrier system. A detector is placed far away from the latter. The (normalized) transmitted intensity $P(\theta)$ recorded by this detector is plotted as a function of the angle (θ) with respect to the normal to the exit plane of the device. To characterize the collimation we calculate $\Delta\theta \equiv |\theta_1 - \theta_2|$ where

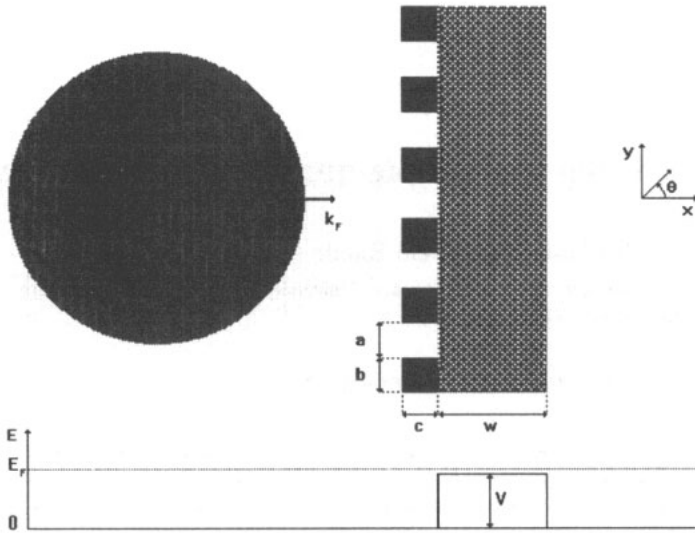


Figure 1. Electron focusing device consisting of quantum point contacts, put in parallel, followed by a tunnelling barrier drawn up by a gate. Also shown is the potential energy diagram along the $(x, y = 0)$ line.

$\theta_{1,2}$ are determined such that the normalized angular distribution $P(\theta_{1,2}) = 1/e$. We define the angular spread $\theta_s \equiv \Delta\theta/2$, because due to the reflection symmetry of the device, $P(\theta)$ for a positive angle of incidence ψ equals $P(-\theta)$ for $-\psi$. The angular distribution $P(\theta)$ thus obtained provides a quantitative characterization of the focusing capability of the device.

To implement this thought experiment, we have simulated the motion of electron waves in the proposed device. The size of the complete system consisting of the emitter, grating+barrier and collector was taken to be $100\lambda_F \times 51\lambda_F$, i.e. comparable to the mean free path of the electrons in 2DEG systems. Incident waves were chosen to be Gaussians of width $6\lambda_F \times 6\lambda_F$, the largest wave packets that can be accommodated by the device. The equation of motion of the electrons, i.e. the time-dependent Schrödinger equation (TDSE), was solved by an accurate and unconditionally stable numerical technique [7]. The TDSE approach is flexible in the sense that it can handle arbitrary geometries and potentials. The angular distribution of the transmitted wave was calculated by the method described in [8]. A typical simulation takes about three hours of CPU time on a CRAY 2-YMP.

A single λ_F -wide quantum point contact is a strong scatterer. This is illustrated by figure 2 which shows the angular distribution for the case of normal incidence ($\psi = 0^\circ$). The angular spread $\theta_s \approx 35^\circ$. In the 2DEG system the electrons impinge on the entrance plane of the point contact from all possible directions. Hence the total angular distribution is an incoherent superposition of distributions for each angle of incidence. Calculations [4,5] for $\psi \neq 0^\circ$ show that for the single point contact θ_s does not significantly depend on ψ , although the shape and the position of the maximum of the angular profile does. Therefore the angular spread of the total angular distribution is larger ($\theta_s \approx 60^\circ$) than the angular spread for normal incidence [4,5]. By putting quantum point contacts in parallel the waves leaving each opening interfere so as to change the angular distribution. This is demonstrated in

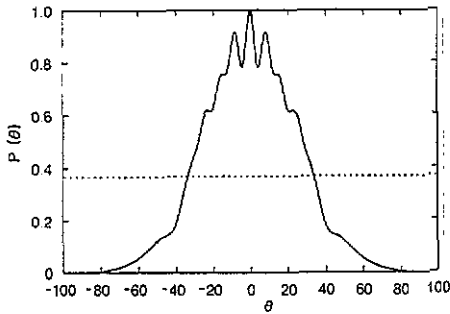


Figure 2. Angular distribution $P(\theta)$ versus angle θ for a wave impinging on a single λ_F -wide constriction. The direction of the incident wave is along the x -axis ($\psi = 0^\circ$). The angular spread $\theta_s \approx 35^\circ$. The dashed line corresponds to $1/e$.

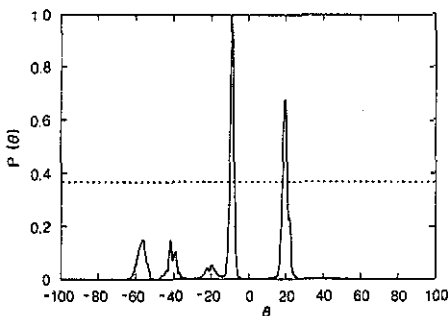


Figure 3. Angular distribution $P(\theta)$ versus angle θ for a wave transmitted by the grating (without barrier, $V = 0$). The angle of incoming wave with respect to the x -axis is $\psi = 20^\circ$. The dashed line corresponds to $1/e$.

figure 3, where we have chosen an angle of incidence $\psi = 20^\circ$. Instead of one broad distribution with some additional structure, the angular distribution now consists of several, rather narrow, peaks. As expected, the current through the grating is, in general, larger than through one of its openings. The grating serves to compress the electron wave but does not, by itself, focus the electron beam in a particular (in our case, normal to the grating) direction. The expression obtained by applying conservation of transverse momentum in the presence of a periodic potential, i.e. $\sin(\theta_{\text{peak}}) = \sin(\theta_{\text{incoming}}) + n/(a + b)$ where $n = 0, \pm 1, \dots$, correctly predicts the positions of all peaks if we take into account the reflections caused by the simulation box boundaries. For instance according to this formula, there should be a peak at $\theta = 57^\circ$ but not at $\theta = -57^\circ$ as indicated in figure 3. This is entirely due to the fact that our simulation box is finite. Those components of the outgoing wave that contribute to the signal at $\theta = 57^\circ$ have already been reflected by the simulation box boundary before the analysis of the wave packet was carried out. The signals at $\theta = -20^\circ$ and $\theta = 41^\circ$, the latter being too weak to show up in figure 3, are also due to reflections by the simulation box boundary. The standard expression for the intensity profile of a grating [9] does not predict the occurrence of the peak at $\theta = -41^\circ$. This is to be expected because the width of each opening is of the order of the wavelength [9].

To eliminate all non-normal components of the outgoing wave as much as possible,

a potential barrier is put behind the constriction(s). The height of the barrier should be chosen such that it is slightly below the Fermi energy E_F and the width of the barrier should be as large as possible (in theory) [4]. Then the potential barrier will reduce the intensity of all transmitted waves with non-zero transverse momentum. In practice the width of the barrier is limited by the size of the device, essentially the distance for ballistic motion. For our calculations presented in this paper we have taken $W = 3\lambda_F$ and $V = 0.98E_F$. The precise values of these parameters are not important as long as they satisfy the qualitative criteria mentioned above. For a device consisting of one constriction only the angular spread, for a wave incident in the normal direction, is reduced considerably (from $\theta_s \approx 35^\circ$ to $\theta_s \approx 10^\circ$) as shown in figure 4. The transmission coefficient $T \approx 0.006$ is much larger than the one of a device proposed earlier [4].

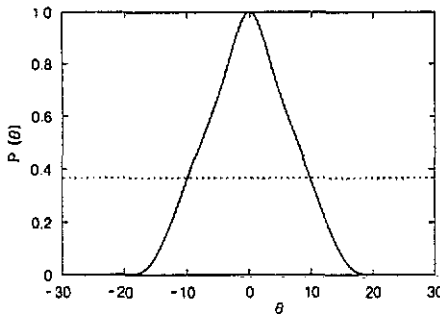


Figure 4. Angular distribution $P(\theta)$ versus angle θ for a wave impinging on a single λ_F -wide constriction followed by the potential described in the text. The direction of the incident wave is along the x -axis ($\psi = 0^\circ$). The angular spread $\theta_s \approx 10^\circ$. The dashed line corresponds to $1/e$.

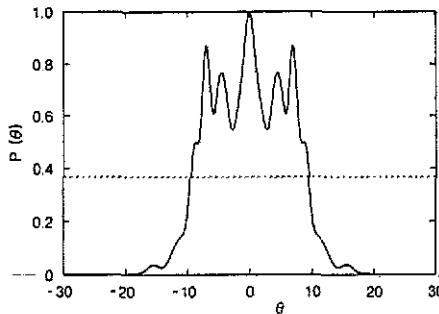


Figure 5. Full angular distribution for the grating+barrier system, obtained by summing over 19 different incoming waves: $\psi = 0^\circ, \pm 2.5^\circ, \pm 5^\circ, \pm 6^\circ, \pm 7.5^\circ, \pm 9^\circ, \pm 16^\circ, \pm 20^\circ, \pm 30^\circ, \pm 50^\circ$. Essentially all intensity is concentrated in a cone of 20° . The dashed line corresponds to $1/e$.

The efficiency of the focusing device can be further enhanced by putting point contacts in parallel, as shown in figure 1. The transmission coefficient for normal incidence $T \approx 0.047$. The full angular distribution of this device is obtained by integrating over all incident waves. In practice we approximate this integral by a

sum over a (small) number of incoming waves. The angular distribution, obtained by summing over 19 different angles of incidence, is depicted in figure 5. The wiggles in $P(\theta)$ are a direct consequence of replacing the integral by a finite sum. Increasing the number of incident waves yields an intensity profile which is smoother but has the same shape. The incoming waves effectively ‘hit’ about six constrictions. The throughput is approximately 0.6%. It is clear that this device is strongly focusing. Unlike for the single-constriction set-up, essentially all transmitted intensity is concentrated in the interval $[-10^\circ, 10^\circ]$. As for all devices of this kind, the focusing effect can be further enhanced by applying an electric field, for instance by changing the Fermi wavelength in the collector of the device [5].

Some remarks about the ‘ideality’ of the device are in order. In our simulations we assumed that the geometry of the device is perfect, made of ideal point contacts. One advantage of having a number of quantum point contacts in parallel may be that conductance fluctuations and localization effects caused by impurities are averaged out [10]. Variation of the width and position of the quantum point contacts reduces the transmission and does not alter the collimation. We now argue that in all respects (excluding imperfections, phonons etc), what we have simulated is a ‘worst case’ situation. In practice the corners of the point contact will be rounded. This rounding leads to an extra collimation of the wave [11–13]. To investigate the influence of smoothening the entrance and exit region of the point contacts, we have attached to the grating horn-like structures but found no noticeable effects. This is in concert with our earlier findings [8] that for constrictions of minimal width $\approx \lambda_F$, rather long horns ($> 5\lambda_F$) are required to improve the focusing. Unlike in the device we have simulated, the potential inside a constriction or grating in a real device will not be zero. It has been suggested [11] that a potential inside a constriction can also provide a mechanism for focusing the wave. Table 1 demonstrates that this is not the case. The diffraction pattern is very similar to that of a constriction without internal potential. Physically, in the absence of a potential behind the constriction, the collimation is determined by the scattering from the exit plane of the constriction, i.e. by a slit. It follows that the two effects mentioned do not significantly improve the focusing. However, they may have influence to the throughput. A potential inside the constriction will reduce the transmission through it, whereas rounding the entrance and exit regions of the grating will increase the transmission coefficient.

Table 1. Influence on the angular spread θ_s of the presence of a constant potential V inside a single λ_F -wide constriction. The angle of incidence $\psi = 0^\circ$.

V/E_F	θ_s
0.00	$34^\circ \pm 4^\circ$
0.75	$34^\circ \pm 4^\circ$
0.98	$33^\circ \pm 4^\circ$
1.00	$34^\circ \pm 4^\circ$

Acknowledgments

We are grateful to N García for a critical reading of the manuscript and for many useful suggestions. We have profited from stimulating discussions with T Klapwijk.

This work is partially supported by the Stichting voor Fundamenteel Onderzoek der Materie (FOM), which is financially supported by the Nederlandse Organisatie voor Wetenschappelijk Onderzoek (NWO), a supercomputer grant of the NCF (The Netherlands), and the EEC Science Plan contract SC1-0395-C (MB).

References

- [1] van Houten H, Beenakker C W J and van Wees B J 1990 *Semiconductors and Semimetals* ed M A Reed (New York: Academic)
- [2] van Houten H, Beenakker C W J, Williamson J G, Broekaart M E I, van Loosdrecht P H M, van Wees B J, Mooij J E, Foxon C T and Harris J J 1989 *Phys. Rev. B* **39** 8556
- [3] Washburn S 1990 *Nature* **343** 415
- [4] De Raedt H, García N and Sáenz J J 1989 *Phys. Rev. Lett.* **63** 2260
- [5] García N, Sáenz J J and De Raedt H 1989 *J. Phys.: Condens. Matter* **1** 9931
- [6] Sivan U, Heiblum M, Umbach C P and Shtrikman H 1990 *Phys. Rev. B* **41** 7937
- [7] De Raedt H 1987 *Comp. Phys. Rep.* **7** 1
- [8] Michielsen K and De Raedt H 1991 *J. Phys.: Condens. Matter* **3** 8247
- [9] Born M and Wolf E 1959 *Principles of Optics: Electromagnetic Theory of Light, Interference and Diffraction of Light* (New York: Pergamon)
- [10] Ismail K, Antoniadis D A and Smith H I 1989 *Appl. Phys. Lett.* **54** 1130
- [11] Beenakker C W J and van Houten H 1989 *Phys. Rev. B* **39** 10445
- [12] Baranger H U and Stone A D 1989 *Phys. Rev. Lett.* **63** 414
- [13] Molenkamp L W, Staring A A M, Beenakker C W J, Eppenga R, Timmering C E, Williamson J G, Harmans C J P M and Foxon C T *Phys. Rev. A* **41** 1247